Eur. Phys. J. A **7**, 79–85 (2000)

THE EUROPEAN PHYSICAL JOURNAL A

EDP Sciences

Cross section and resonance strength measurements of ^{19}F(p,$\alpha\gamma$)^{16}O at E$_p$ = 200–800 keV

K. Spyrou[1], C. Chronidou[1], S. Harissopulos[1], S. Kossionides[1], T. Paradellis[1], C. Rolfs[2], W.H. Schulte[2], L. Borucki[2]

[1] N.C.S.R. "Demokritos", Institute of Nuclear Physics, Laboratory for Material Analysis, 153.10 Athens, Greece
[2] Institut für Physik mit Ionenstrahlen, Ruhr-Universität-Bochum, Universitätsstrasse 150, 44780 Bochum, Germany

Received: 21 June 1999 / Revised version: 30 September 1999
Communicated by D. Schwalm

Abstract. An excitation function of the ^{19}F(p,$\alpha\gamma$)^{16}O reaction has been measured over the proton beam energy range E$_p$=200-800 keV using a 4π NaI summing spectrometer. A new resonance was found at E$_R$=237 keV and its properties Γ_R, σ_R and $\omega\gamma$ have been extracted. The strengths of all resonances at E$_p$ = 200 - 800 keV have been also extracted. The importance of the 1$^+$ resonance at E$_R$=11 keV is discussed and its width has been estimated taking into account interference effects with the strong 1$^+$ resonance at E$_R$=340 keV. The reaction rates have been calculated over a wide range of temperatures and compared with the rates of the (p,α_0) and (p,α_π) branches of the ^{19}F(p,α)^{16}O reaction.

1 Introduction

The importance of the ^{19}F(p,α)^{16}O reaction in nuclear astrophysics has been discussed by Rolfs and Rodney [1]. The ^{19}F(p,$\alpha\gamma$)^{16}O branch of this reaction dominates the reaction rate over a wide temperature range and especially at high temperatures relevant to hot and explosive hydrogen burning. Given its importance, a precise and complete measurement of the total cross section appeared desirable. The energy range E$_p$=800-3600 keV (all energies are given in the laboratory system, except where quoted differently) has been studied previously [2] using a 4π NaI detection system, where the strength $\omega\gamma$ for narrow resonances and the astrophysical S-factor for broad resonances have been obtained.

In the present work the studies have been extended to low energies, E$_p$ $\leq$800 keV, using a similar detection system. The results from previous and present work allow to calculate the reaction rates over a wide range of temperatures.

2 Experimental setup and procedures

Proton beams (with up to 2 μA current on target) have been provided by the 450 kV accelerator and the 4 MV tandem accelerator of the Dynamitron Tandem Laboratorium at the Ruhr-Universität Bochum. The experimental setup is shown schematically in Fig. 1. The proton beam was focussed to a spot of about 4 mm diameter on the target after passing through the apertures A$_1$ and A$_2$ (distance 103 cm) which had a diameter of 6 and 3 mm, respectively. The air cooled target was placed at a 62 cm distance from aperture A$_2$ cylindrical stainless steel target chamber of 50 cm length, 32 mm inner diameter, and a 0.5 mm wall thickness. The target chamber was electrically insulated from the beam line via a metal-ceramic flange and served as Faraday cup for beam integration. A second metal-ceramic flange served to insulate aperture A$_2$ from A$_1$. The beam currents measured at A$_1$, A$_2$, and the Faraday cup were used to optimize the beam profile on target. Hereby, a voltage of -300 V was applied to the part of the beam tube between the two metal-ceramic flanges in order to supress the effects arising from secondary electron emission. In order to avoid carbon-buildup on target, the setup was equiped with a liquid-nitrogen cooled in-line Cu tube of 50 cm length. With this tube, the metal-sealed UHV components of the setup, and the operation of a turbo pump with 360 l/s pumping speed, a base pressure of 1.2$\times$ 10^{-8} mbar was achieved.

The γ-rays have been detected by a 12 inch $\times$ 12 inch NaI(Tl) crystal with a central borehole of 35 mm diameter and a 0.5 mm Al wall thickness. The crystal could be moved on a rolling tray so that the target could be placed at the center of the crystal. Due to the 4π geometry covered by the summing crystal, the detected γ-rays are angle integrated leading to the ability of measuring directly the total cross section.

Three γ-rays of energy 6130, 6917 and 7117 keV are expected in the ^{19}F(p,$\alpha\gamma$)^{16}O reaction which correspond to the (p,α_2), (p,α_3), and (p,α_4) branches, respectively. The ^{19}F(p,α_1)^{16}O reaction is followed by the emission of

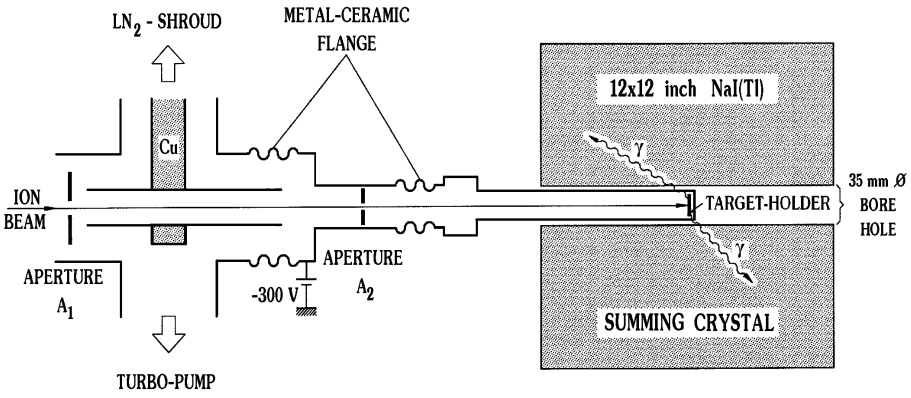

Fig. 1. Schematic diagram of the experimental setup

e^+-e^- pair. The notation is $^{19}F(p,\alpha_\pi)^{16}O$. Most of the resonances at E_p = 200 - 800 keV deexcitate predominantly through the (p,α_2) branch. A typical spectrum of the reaction is shown in Fig. 2.

3 Analysis and results

3.1 Excitation functions and resonance strengths

The excitation function of the $^{19}F(p,\alpha\gamma)^{16}O$ reaction has been obtained at E_p=200-800 keV. The energy steps varied from 1 keV (when scanning a resonance) to 10 keV. The spectrum integration window was 4.2 MeV to 9 MeV. The absolute detection efficiency ϵ of the summing crystal was measured over a wide range of γ-energies [3], where the results have been in good agreement with Monte Carlo simulations using the code GEANT. At the relevant energy range, E_γ=6.13-7.11 MeV, ϵ is nearly constant. If the integrated window includes part of the low-energy tails, one finds [3] ϵ=0.73 $\pm$ 0.06 for an integration window 3 MeV to 9 MeV. The adaptation to the present situation, i.e. integration window 4.2-9.0 MeV was performed with a spectrum taken at the E_p=872 keV resonance [2] yielding $\varepsilon = 0.69 \pm 0.06$. Dead time effects were accounted for. The accumulated charge at the target varied between 0.5 and 10 μCb with an estimated error of 3%. The background from the Cu backing of the target was measured by bombarding a single Cu backing and has been accounted for.

The experiments were carried out using three thin fluorine targets, all of them produced at the Dynamitron Tandem laboratory at the Ruhr-Universitat Bochum by evaporating natural CaF_2 powder on a clean Cu backing. In addition some resonances were investigated using a thick fluorine target which was produced at the Institute of Nuclear Physics at N.C.S.R. "Demokritos", by evaporating natural CaF_2 powder on a clean W backing. The thin targets were used to obtain the excitation function stepwise for proton energies E_p=417-800, 217-435, and 200-223 keV. To check for possible deteriorations of the targets due to bombardment, tests were made frequently by scanning the nearest resonance and checking the yield at the maximum and the observed width. Only for the third target and after bombardment with high currents a 5% reduction in yield was observed at the two last measured points, which is within the experimental errors.

The excitation functions which correspond to the three above mentioned sets of data are shown in Fig. 3, where

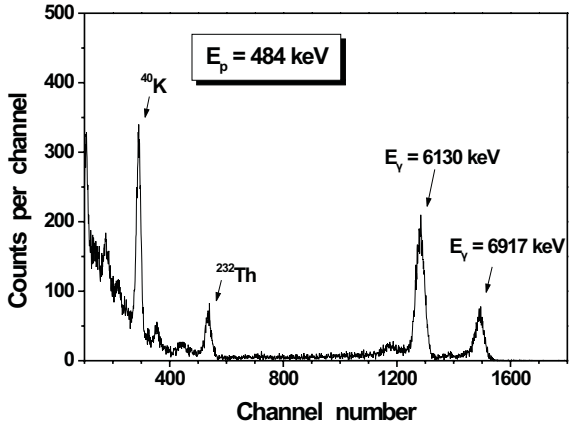

Fig. 2. A γ-ray spectrum obtained with the summing crystal for the $^{19}F(p,\alpha\gamma)^{16}O$ reaction at E_p=484 keV

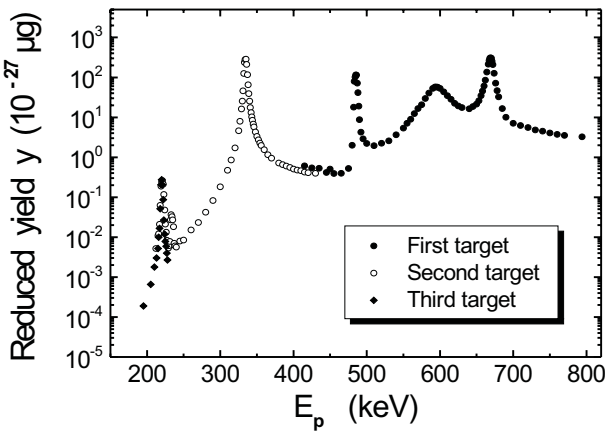

Fig. 3. Excitation function of $^{19}F(p,\alpha\gamma)^{16}O$ obtained with three thin targets

the energies are not corrected for the energy offset of the proton beam. The excitation functions are expressed in terms of the reduced reaction yield which is defined as the ratio of the integrated number of counts C for all the three transitions over the number of incident protons N_p, the detection efficiency ε and the number of target atoms per gramm N_A/A, where N_A is the Avogadro number and A the atomic weight of fluorine

$$y = C/(\varepsilon \cdot N_p \cdot N^*) = \sigma \cdot dx_F \ , N^* = N_A/A \qquad (1)$$

The cross section σ is expressed in mb and the infinitesimal fluorine thickness of the target dx_F in μg/cm^2. Thus, the reduced yield y is in $10^{-27}\mu$g.

If the target has a finite total thickness x, the corresponding energy loss for proton energy E_p is $\Delta_{lab}(E_p) = T(E_p) \cdot x$, where $T(E_p)$ is the stopping power of protons for the target materials. In the present work the stopping power values are obtained from Andersen and Ziegler [4]. In case the target has a finite total thickness x, the reduced reaction yield becomes an integral over the target thickness :

$$y(E_p) = p_F \cdot \int_0^x \sigma(E) \cdot dx = p_F \cdot \int_{E_p - \Delta_{lab}}^{E_p} \frac{\sigma(E)}{T(E)} dE \quad (2)$$

where p_F is the fluorine weight proportion in the target. The cross section of an isolated narrow resonance is given by the Breit-Wigner formula:

$$\sigma(E) = \sigma_R \cdot \frac{E_R}{E} \cdot \frac{\Gamma_R^2}{4 \cdot (E - E_R)^2 + \Gamma_R^2} \qquad (3)$$

At energies far away E$_R$, the energy dependence of the partial and total widths must be included [1].

The reaction yield is influenced by the beam energy distribution and the energy straggling of protons inside the target. The standard deviation of the straggling distribution is described sufficiently well by Bohr's formula [5]

$$\Omega_B = \left(0.156 \cdot z^2 \cdot \frac{\overline{Z}}{\overline{A}} \cdot x\right)^{1/2} (keV) \qquad (4)$$

where x is in μg/cm^2, $\overline{Z}$ and $\overline{A}$ are the average atomic and mass numbers, respectively, and z is the atomic number of the projectile. The total energy distribution is the result of contributions from straggling and from the intrinsic energy spread of the beam Δ_b. Both effects have been included in a single gaussian function [6] in order to avoid a triple integral and to simplify the calculations, namely

$$g(E_p, E', x) = B \cdot exp\left[-\frac{(E_p - E' - T(E_p) \cdot x)^2}{0.36 \cdot \Gamma_t^2}\right] \qquad (5)$$

where B is the normalization constant and Γ_t is the total FWHM of the energy spreading:

$$\Gamma_t = \left(\Delta_b^2 + 0.86 \cdot z^2 \cdot \frac{\overline{Z}}{\overline{A}} \cdot x\right)^{1/2} \qquad (6)$$

Consequently, the reduced reaction yield is given by the double integral :

$$y(E_p) = \sigma_R \cdot p_F \cdot \int_0^x \int_0^\infty \frac{E_R}{E'} \cdot \frac{\Gamma_R^2}{4 \cdot (E' - E_R)^2 + \Gamma_R^2} \cdot \cdot g(E_p, E', x) \cdot dE' \cdot dx \qquad (7)$$

or $y(E_p) = \sigma_R \cdot p_F \cdot x_{eff}(E_p; \Gamma_R, E_R, x)$.

The resonant yield can be calculated using formula (7) by performing numerical integration, if the resonance properties E_R, Γ_R and σ_R as well as the thickness x and composition p$_F$ of the target are known. Moreover, the experimental resonance yield can be fitted using the above expression for the determination of some of the variables.

In the case where the target is thin and the cross section varies smoothly with energy the cross section can be extracted from the thin target relation

$$y = p_F \cdot x \cdot \sigma \qquad (8)$$

using an effective beam energy of

$$E_{eff} = E_p - \Delta_{lab}(E_p)/2 \qquad (9)$$

which accounts for the target thickness.

The $E_R = 340$ keV resonance has been used to determine the parameters of the target which served to obtain the excitation function for E$_p$=217-430 keV. Since the energy and width of this resonance are well known [7], the experimental yield of the 340 keV resonance has been fitted using formula (7) and having as free fit parameters the target thickness x, the weight proportion of fluorine p_F, and the cross section σ_R. The results are : $x = 9.0 \pm 0.9$ μg/cm^2, p$_F$ = 0.54$\pm$0.05 and $\sigma_R = 93 \pm 10$ mb. The result for the cross section is in excellent agreement with the literature value [8], $\sigma_R = 91 \pm 4$ mb. The literature value is derived by dividing the quoted (p, α_2) cross section with its branching ratio of 0.97 [9]. The resonance strength was calculated using [1] the relation

$$\omega\gamma = \mu \cdot E_R^{cm} \cdot \sigma_R \cdot \Gamma_R^{cm}/(2\pi\hbar^2) \qquad (10)$$

where μ is the reduced mass. Using the above result for the cross section and the literature values for E$_R$ and Γ_R, the strength was found to be $\omega\gamma = 24.3 \pm 2.8$ eV

In the case of the E$_R$=224 keV resonance, the yield contribution from the 340 keV resonance near E$_R$=240 keV was calculated using formula (7) and then subtracted from the experimental yield of the 224 keV resonance prior to the fitting procedure. Penetration coefficients for entrance and exit channels were included in the calculation of the 340 keV resonance. Using the well known energy and width of 224 keV resonance [7] together with the above results for x and p$_F$, the result for the cross section was $\sigma_R = 167 \pm 23$ μb leading to a resonance strength $\omega\gamma = 12.2 \pm 1.7$ meV. In the literature the only estimation for this resonance is $\sigma_R \geq 200$ μb [10]. Accordingly, a level with $J^\pi = 1^+$ observed by Betts *et al.* [11] at an excitation energy of 12823 keV was reassigned an energy value of 12859 keV, corresponding to a resonance E$_R$=11.6 keV in the ^{19}F(p,α)^{16}O reaction.

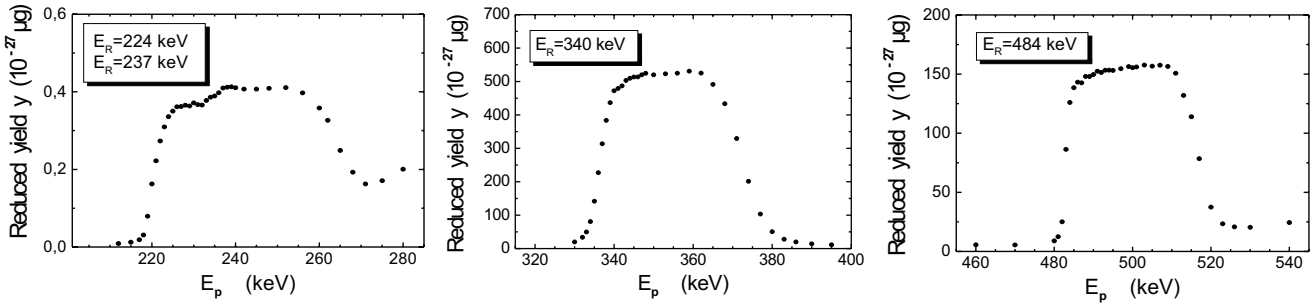

Fig. 4. Thick target yield for four resonances of the ^{19}F(p,$\alpha\gamma$)^{16}O reaction a) E$_R$=224 and 237 keV b) E$_R$=340 keV and c) E$_R$=484 keV

A new resonance (see Fig. 4) is observed at the proton energy E$_R$=237 keV corresponding to an excited level of ^{20}Ne at E$_x$=13073 keV, which has been previously observed in the ^{19}F(^{3}He,d)^{20}Ne reaction by Kious [12]. Kious has performed an accurate analysis of this reaction and concluded that there was a systematic difference of 36 keV between his data and the corresponding data of Betts *et al.* [11]. As a result, the 13037 keV level of Betts *et al.* corresponds to a 13073 keV level (E$_R$=237 keV) with $J^\pi = 3^-$.

The new resonance at E$_R$=237 keV decays via the α_2 branch leading to the emission of 6130 keV photons as has been checked from the spectra corresponding to the resonance peak. In order to determine its parameters calculations of the expected experimental yield of the 340 keV and 224 keV resonances were initially performed using formula (7) and then subtracted from the experimental yield of the resonance prior to the fitting procedure. The final results are E$_R$ = 237.0 ± 0.5 keV, $\Gamma_R = 0.39 \pm 0.15$ keV and $\sigma_R = 41 \pm 16$ μb, leading to a resonance strength $\omega\gamma = 1.2 \pm 0.7$ meV. From the quoted spectroscopic factor by Kious [12] for the 13073 keV level we calculate $\omega\gamma \approx 0.2$ meV, a factor of 4 less than the presently measured value. The strengths of the 224 keV and 237 keV resonances (and the 484 keV resonance as well) have been extracted independently via a thick target measurement (Fig. 4), relative to the thick target measurement of the 340 keV resonance (Fig. 4).

The resonance strength is related to the thick target yield [1] by the equation:

$$y_\infty = \frac{\lambda^2}{2}\omega\gamma\frac{M+m}{M}\frac{1}{T}\frac{1}{p_F} \qquad (11)$$

where m and M are the projectile and target masses, respectively. For two resonances measured with the same target, the relation between the strengths and the thick target yields is

$$\frac{\omega\gamma_1}{\omega\gamma_2} = \frac{y_1^\infty}{y_2^\infty}\frac{E_{R,1}}{E_{R,2}}\frac{T(E_{R,1})}{T(E_{R,2})} \qquad (12)$$

Having as standard the 340 keV resonance and its present strength value and using formula (12) the strengths of the 224 keV and 237 keV resonances have been extracted as $\omega\gamma = 13.2 \pm 1.9$ and $\omega\gamma = 1.1 \pm 0.6$ meV, respectively, leading to the respective average values $\omega\gamma = 12.6 \pm 1.3$ and $\omega\gamma = 1.1 \pm 0.4$ meV (Table 1).

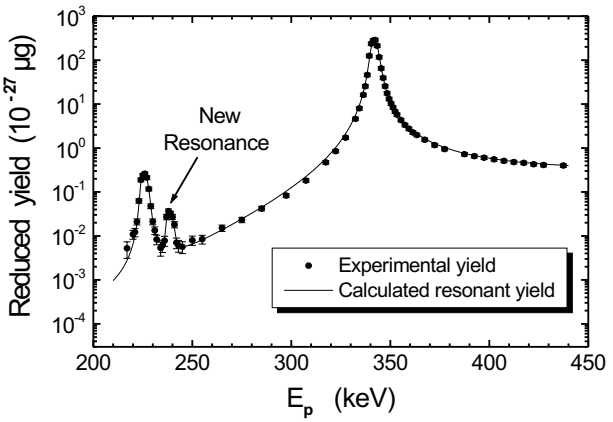

Fig. 5. Excitation function of the ^{19}F(p,$\alpha\gamma$)^{16}O reaction at E$_p$=217-435 keV. The solid curve is the sum of the calculated resonant yields of the narrow resonances at E$_R$=224, 237 and 340 keV using the present fit results

The expected yield due to the three resonances is shown in Fig. 5 (solid line), calculated using formula (7) and the present results. The first resonance in the realm of higher energies, the 484 keV resonance, could be investigated with the thick target method, as detailed above yielding $\omega\gamma = 8 \pm 1$ eV. The other resonances in the realm E$_p$=417-800 keV were investigated with a thin target. Its properties were determined as follows: The excitation function at E$_p$=417-800 keV has a common energy region with the excitation function at E$_p$=217-435 keV (Fig. 3). The cross section in this common region varies slowly with energy.

Thus, by comparing the yield from the two measurements one compares the fluorine thickness $x_F = p_F x$ of the target (8). The target for E$_p$=417-800 keV was found to have $x_F = 6.5 \pm 0.6$ μg/cm^2. Moreover, the yield curve at the E$_p$=872 keV resonance was measured and the experimental yield been fitted on the basis of formula (7) as described in [2]. The target thickness was found to be $x = 13.0 \pm 1.2$ μg/cm^2.

The resonance at E$_R$=594 keV [13,14] is a broad resonance. Thus, the cross section σ_R can be deduced directly

Table 1. Results for the ^{19}F(p,$\alpha\gamma$)^{16}O resonances

		Present Work		Literature		
E$_R$ [a] (keV)	Γ_R [a] (keV)	σ_R (mb)	$\omega\gamma_{cm}$ (eV)	σ_R [e] (mb)	σ_R [f] (mb)	$\omega\gamma_{cm}$ (eV)
11.6±0.5[b]	0.03(2-120eV)[c]		8.5×10^{-29}[d]			
224.99±0.07	0.99±0.02	0.173±0.018	0.0126±0.0013		≥0.2	
237.0±0.5 [c]	0.39±0.15 [c]	0.041±0.016	0.0011±0.004			0.0002 [g]
340.46±0.04	2.34±0.04	93±11	24.3±2.9	59	160	23.0±0.8 [h]
483.91±0.10	0.9±0.03	56±7	8±1	29	≥32	
594.4±0.9	27.5±2.5	8.9±1.1	48±7	4	7.1	
669.0±0.7	6.6±0.28	52±6	75±9	25	57	

[a] [7,13,14]
[b] [11,12]
[c] Present Work
[d] Present calculation using spectroscopic factors from [11,12]
[e] [15]
[f] [10]
[g] [12]
[h] [8]

using formula (8): $\sigma_R = 8.9\pm1.1$ mb. Using the energy and width from the literature [13,14] the resonance strength is calculated as $\omega\gamma = 48\pm 7$ eV. The cross section for the E$_R$=669 keV resonance was determined via a fitting process to the experimental yield of the resonance using formula (7). The result is $\sigma_R = 52\pm6$ mb. Using the energy and width from literature [13,14] the resonance strength is calculated as $\omega\gamma = 75\pm 9$ eV. The results for all the resonances are summarized and compared with literature values in Table 1.

3.2 The E_R^{cm}=11 keV resonance

As a result of the ^{19}F(^{3}He,d)^{20}Ne work by Kious [12] the existence of a E_R^{cm}=11 keV resonance with $J^\pi = 1^+$ and spectroscopic factor S$_p$=0.056. This level is also reported by Betts *et al.* [11] with $J^\pi = 1^+$ and S$_p$=0.05, but situated 25 keV below threshold.

Using the spectroscopic factor, the width for the entrance channel has been calculated via the following relation as given in [1],

$$\Gamma_p = 2\gamma^2 P_l(E) C^2 S_p \qquad (13)$$

with C^2 being the square of the isospin Clebsh-Gordan coefficient with value 1/2, $P_l(E)$ the penetration factor for proton angular momentum l and

$$\gamma^2 = \frac{4.18}{\mu R_n^2}(MeV) \qquad (14)$$

the Wigner limit with $R_n = 1.4(A_1^{1/3}+A_2^{1/3})$. For E_R^{cm}=11 keV, S_p=0.053 and $l = 0$, equation (13) gives a width of $\Gamma_p = 1.14\times10^{-28}$ eV. Since $\Gamma_p \ll \Gamma_\alpha$, the width for the exit channel Γ_α is equal to the total width Γ, and the resonance strength is given by $\omega\gamma = \omega\Gamma_p\Gamma_\alpha/\Gamma = \omega\Gamma_p$. Since ω=3/4, a value of $\omega\gamma = 8.5\times10^{-29}$ eV results for the strength of the E_R^{cm}=11 keV resonance.

The existence of this $J^\pi = 1^+$ resonance may affect the behavior of the S-factor at low energies due to interference effects with the strong 1^+ resonance at E$_R$=340 keV and all the other 1^+ resonances. In the work of Kious [12], possible interference effects have been discussed and a R-matrix analysis has been performed. Kious concluded that S-factor below the 340 keV resonance is affected mainly by the destructive interference between E_R^{cm}=11 keV and E$_R$=340 keV resonances and that the width of the E_R^{cm}=11 keV resonance may vary between 2 eV and 1 keV. The latter value introduces large uncertainties to the astrophysical S-factor below E$_p$=200 keV.

A thin target was used in order to measure the excitation function as low as possible. The 224 keV resonance was scanned (Fig. 3) in order to extract the parameters of this target: $x_F = 3.4\pm0.4\mu$g/cm^2 and $x = 5.1\pm0.5\mu$g/cm^2 and $p_F = 0.67\pm0.07$ The reaction yield was measured at E$_p$=200, 210, and 215 keV. For these three points the cross section and the corresponding effective energy have been extracted using equations (8) and (9). The astrophysical S-factor was then calculated using [1] the expression

$$S(E_{cm}) = \sigma(E_{cm})\cdot E_{cm}\cdot exp(275.49\cdot E_{cm}^{-0.5}) \qquad (15)$$

with E$_{cm}$ in units of keV. The same analysis was performed for 9 experimental points which lay in the interval between the 244 keV and 340 keV resonances and which have been obtained with the second, thin target used for E$_p$=217-430 keV (Fig. 5). The results for the 12 points are presented in Table 2 and displayed in Fig. 6.

Assuming interference effects between the E_R^{cm}=11 and 323 keV resonances the experimental points have been fitted using the expression

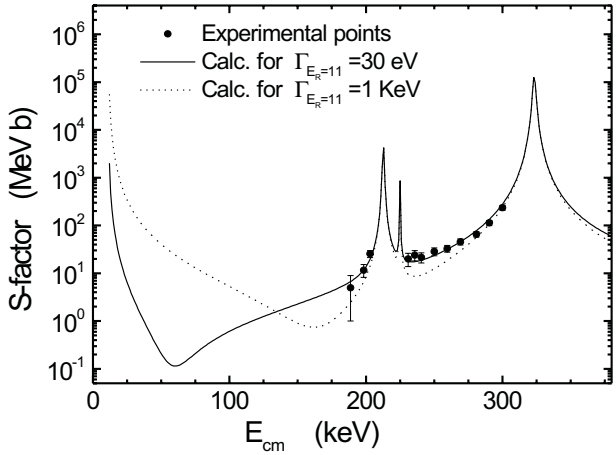

Fig. 6. Experimental and calculated S-factor, assuming interference effects between the E$_R^{cm}$=11 and 323 keV resonances

Table 2. Astrophysical S-factor as a function of center of mass energy E$_{cm}$

E$_{cm}$(keV)	S(MeV·b)
188.8	5 ± 4
198.3	12 ± 3
203.1	26 ± 4
231.0	20 ± 6
235.8	24 ± 6
240.5	22 ± 5
250.1	29 ± 5
259.6	33 ± 5
269.1	46 ± 6
280.9	66 ± 8
290.4	114 ± 14
299.9	235 ± 28

$$S(E) = \sum_{i=1}^{7} S_{R_i}(E) - 2(S_{R_1}(E)S_{R_4}(E))^{1/2} \cdot cos(\delta_{R_1}(E) - \delta_{R_4}(E)) \quad (16)$$

where S$_{R_i}$(E) are the S(E) factors of the seven resonances at E$_R$=11, 224, 237, 340, 484, 594 and 669 keV, calculated using the present results and taking into account the energy dependence of the penetration coefficients for the entrance and exit channels. The phase shifts δ_{R_1} and δ_{R_4} of the two interfering resonances are described by

$$\delta_{R_i}(E) = arctan(\frac{\Gamma_{R_i}}{2(E - E_{R_i})}) \quad (17)$$

The only free fit parameter was the width of the 11 keV resonance. The lowest χ^2 was achieved for the value Γ_R=30 eV. Taking into account the error resulting from the fit and the variation of χ^2, a safe interval 2-120 eV is recomended for the width of the 11 keV resonance. In Fig. 6 the calculation of the S-factor using formula (16) is shown for two widths: Γ_R=30 eV (solid curve) and Γ_R=1 keV (dotted curve).

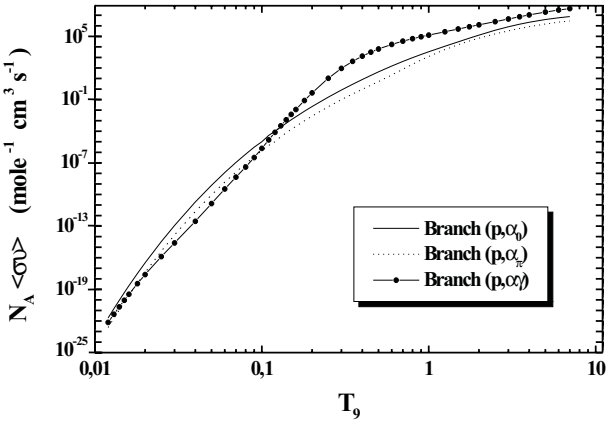

Fig. 7. Reaction rate for the three branches of the $^{19}F(p,\alpha)^{16}O$ reaction (T$_9$ in units of 10^9 K)

3.3 Reaction rate calculations

The reaction rate $N_A < \sigma v > (mole^{-1} \cdot cm^3 s^{-1})$ [1] vs. temperature for the (p,$\alpha\gamma$) branch of the ^{19}F(p,α)^{16}O reaction has been calculated using the present results and the previous results at E_p=800-3600 keV [2]. The results are shown in Fig. 7. All different contributions to the rate have been taken into account and have been computed independently [1], namely, the resonance terms, the resonance tails at low energies and the direct maxwellian-averaged integration of the S-factor at low and high energies. The low energy S-factor assumed the calculated interference pattern between the E$_R$=11 keV and E$_R$=340 keV resonances.

Moreover, the reaction rates of the (p,α_0) and (p,α_π) branches have been calculated using literature data and are shown in Fig. 7. The data used have been taken from the NACRE compilation [16]. The (p,$\alpha\gamma$) branch of the reaction is dominant at high temperatures (T$_9$ $\geq$0.1), while the (p,α_0) branch is dominant at low temperatures. The resulting total ^{19}F(p,α)^{16}O reaction rate is in excellent agreement with the NACRE compilation [16].

4 Conclusions

Present work completes the quantitative information on the total cross section for the ^{19}F(p,$\alpha\gamma$)^{16}O reaction. The results have been presented in terms of the resonance strength $\omega\gamma$ for all the observed resonances below E$_p$=800 keV. The new resonance at 237 keV corresponds to a 13070 keV state in ^{20}Ne observed previously via the ^{19}F(^{3}He,d) reaction. Moreover, there is strong evidence suggesting that the width of the 11 keV resonance is lower than 120 eV with a most probable value of Γ_R=30 eV. This reduces the uncertainties of the S-factor in the energy region E$_p$ $\leq$ 200 keV and hence reduces also the uncertainties of the reaction rate which existed due to the lack of experimental information at low energies. Reaction rate calculations using results from the present work, [2] and the NACRE compilation [16], have been performed and

confirmed the dominance of the (p,α_0) branch at temperatures below T$_9$=0.1.

References

1. C. Rolfs, W.S. Rodney, Cauldrons in the cosmos (University of Chicago Press, 1988)
2. K. Spyrou, C. Chronidou, S. Harissopulos, S. Kossionides, T. Paradellis, Z. Phys. **A357**, 283 (1997)
3. M. Mehrhoff, Diplomarbeit, Ruhr-Universität-Bochum (1996)
4. H.H. Andersen and J.F. Ziegler, *Hydrogen Stopping Powers and Ranges in All Elements*, Vol. 3, (New York: Pergamon Press, 1997)
5. N. Bohr, Philoshophical Magazine **30**, 581 (1915)
6. G. Deconninck, Introduction to Radioanalytical Physics (Akademiai Kiado, 1978)
7. M. Uhrmacher, K. Pampus, F. J. Bergmeister, D. Purschke, K. P. Lieb, Nucl. Instr. Meth. **B9**, 243 (1985)
8. H. W. Becker, W. E. Kieser, C. Rolfs, H. P. Trautvetter, M. Wiescher, Z. Phys. **A305**, 319 (1982)
9. S. Croft, Nucl. Instr. Meth. **A307**, 353 (1991)
10. C. Y. Chao, A. V. Tollestrup, W. A. Fowler, C. C. Lauritsen, Phys. Rev. **79**, 108 (1950)
11. R. R. Betts, H. T. Fortune R. Middleton, Phys. Rev. **C11**, 19 (1975)
12. M. Kious, Ph.D thesis, Universite de Paris XI (1990)
13. S. E. Hunt, K. Firth, Phys. Rev. **99**, 786 (1955)
14. D. Dieumegard, B. Maurel, G. Amsel, Nucl. Instr. Meth. **168**, 93 (1980)
15. T. W. Bonner, J. E. Evans, Phys. Rev. **73**, 666 (1948)
16. **N**uclear **A**strophysics **C**ompilation of **RE**action Rates (**NACRE**) C. Angulo, M. Arnould, M. Rayet, P. Descouvemont, D. Baye, C. Leclerq-Willain, A. Coc, S. Barhoumi, P. Auger, C. Rolfs, R. Kunz, J.W. Hammer, A. Mayer, T. Paradellis, S. Kossionides, C. Chronidou, K. Spyrou, S. Degl'Innocenti, G. Fiorentini, B. Ricci, S. Zavaratelli, C. Providencia, H. Walters, J. Soares, C. Crama, J. Rahighi, A. Shotter, M. Lamehi Rachti, Nucl. Phys. **A656**, 3 (1999)